An efficient response sensitivity analysis method for a bounding surface plasticity sandy soil model

Q. Gu

Xiamen University, Xiamen, Fujian, China

G. Wang

Hong Kong University of Science and Technology, Hong Kong

S. Huang

Xiamen University, Xiamen, Fujian, China

ABSTRACT: Finite element (FE) response sensitivity analysis is an important component in gradient-based algorithms, such as structural optimization, reliability analysis, system identification, and FE model updating. In this paper, the FE response sensitivity analysis methodology based on the direct differentiation method (DDM) is applied to a bounding surface plasticity material model that has been widely used to simulate nonlinear soil behaviors under static and dynamic loading conditions. The DDM-based algorithm is derived and implemented in a general-purpose nonlinear finite element analysis program OpenSees. The algorithm is validated through simulation of the nonlinear cyclic response of a multilayered soil ground in ?? subjected to liquefaction under earthquake loading. The response sensitivity results are validated and compared with those from Forward Finite Difference (FFD) analysis. Furthermore, the results are used to determine the relative importance of various soil constitutive parameters to the dynamic responses of the system. The DDM-based algorithm is demonstrated to be accurate and efficient in computing the FE response sensitivities, and has great potential in the sensitivity analysis of highly nonlinear soil-structure systems.

1 INTRODUCTION

1.1 *Background*

Finite element (FE) response sensitivity analysis is an essential ingredient of gradient-based optimization methods and is required in structural optimization, system identification, reliability, and FE model updating (Kleiber et al. 1997, Conte et al. 2003). Furthermore, the sensitivity analysis results may be used to quantify the material and loading uncertainty and its propagation from original sources to the structural responses of interest. In addition, FE response sensitivities provide invaluable insight into the effects of system parameters on, and their relative importance to the system response (Gu et al. 2009). Several methods are available for response sensitivityanalysis, including the Finite Difference Method (FDM), the Adjoint Method (AM), the Perturbation Method (PM), and the Direct Differentiation Method (DDM) (Zhang & Der Kiureghian 1993, Gu et al. 2009, Scott et al. 2004, Haukaas et al. 2006). The FDM is the simplest method for response sensitivity computation, but is computationally expensive and can be negatively affected by numerical noise. The AM is efficient for linear and non-linear elastic systems, but is not a competitive method for path-dependent (i.e., inelastic) problems. The PM is computationally efficient although generally not very accurate. The DDM, on the other hand, is a general, accurate and efficient method that is applicable to any material constitutive model. The DDM-based response sensitivity analysis methodology shows great promise in the analysis of complicated structural or geotechnical systems.

However the DDM method requires the analytical derivation and numerical implementation to differentiate the system responses with respect to sensitivity parameters. Over the past decade, the DDM-based sensitivity analysis method has been actively developed and implemented in an open source FE analysis framework known as OpenSees (Mckenna & Fenves, 2001). The DDM has been developed for various constitutive models including uniaxial materials, three-dimensional J_2 plasticity models and pressure-independent multi-yield surface J_2 plasticity models (Fu el al. 2010). These models can be used to simulate truss and beam components in the structures, and nonlinear clay behaviors. Detailed descriptions of the DDM-based sensitivity analysis methodology implemented in OpenSees can be found in the literature (Der Kiureghian & Haukaas 2006, Gu 2008).

Recently the method has been formulated for sandy soils, which usually exhibit different behaviors from clayey soils, such as pressure-dependent cyclic behaviors, shear-induced volumetric dilation and contraction, as well as flow liquefaction under low effective confinement. The objective of this paper is to summarize the DDM-based sensitivity analysis to a class of bounding surface models for sandy soils. The bounding

surface model has been widely used and proven to be an effective and robust model to simulate the behaviors of sandy materials under cyclic and seismic loading conditions (Dafalias 1986, Li 2002). The DDM-based sensitivity algorithm is particularly efficient for strongly nonlinear, large-scale problems with a large number of sensitivity parameters. The geotechnical problems modeled by the bounding surface model are an example. Thus developing a DDM sensitivity algorithm for the bounding surface model will allow us to solve a large number of challenging geotechnical problems, such as the earthquake-induced liquefaction phenomenon in sandy soils. When combined with the existing sensitivity analysis framework for clayey soils and soil-structure interaction systems, the DDM-based sensitivity analysis may be readily applied to real soil-foundation-structure interaction systems (Gu 2008).

This paper provides a brief summary of the bounding surface model and DDM formulation, followed by an example to validate the DDM-based response sensitivity algorithm. The algorithm is applied to study the sensitivity of liquefied ground responses at Port Island in Japan under a real earthquake scenario. The results are further used to identify the relative importance of the soil parameters to the surface responses.

1.2 *Numerical implementation of a bounding surface model*

The bounding surface model employs a stress ratio invariant, defined as $R=\sqrt{0.5\mathbf{r}:\mathbf{r}}$, where $\mathbf{r}$ is the stress ratio of the deviatoric stress $\mathbf{s}$ over pressure p, i.e., $\mathbf{r}=\mathbf{s}/p$, and the notation "**:**" is the double contraction between two second-order tensors, i.e., **A:B** = $A_{ij}B_{ij}$. Accordingly, an ultimate failure surface, or a failure-bounding surface, is defined as: $\hat{f}=\hat{R}-R_f=0$, where the hats "^" denote stress quantities on failure surface, the parameter R_f is the stress ratio invariant at the failure surface, which is related to the corresponding classical critical state triaxial parameter M by $R_f=M/\sqrt{3}$, and the parameter interpolates between compression and extension. Similarly, the maximum prestress memory bounding surface is defined as: $\bar{f}=\bar{R}-R_m=0$, where R_m is a history parameter providing the maximum prestress level. The two bounding surfaces are combined to compute the plastic modulus, as shown in Fig. 1.

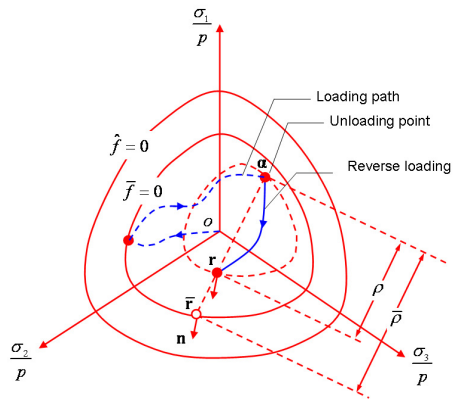

Figure 1. Model mechanism in deviatoric stress ratio space

Inside the failure-bounding surface, the hypoelastic response, i.e., the elastic strain rate $\dot{\boldsymbol{\varepsilon}}^e$, is defined as the summation of deviatoric strain $\dot{\mathbf{e}}^e$ and volumetric strain $tr\dot{\boldsymbol{\varepsilon}}^e$ as:

$$\dot{\boldsymbol{\varepsilon}}^e=\dot{\mathbf{e}}^e+\frac{1}{3}(tr\dot{\boldsymbol{\varepsilon}}^e)\mathbf{I}=\frac{1}{2G}\dot{\mathbf{s}}+\frac{1}{3K}\dot{p}\mathbf{I} \qquad (1)$$
$$=\frac{1}{2G}p\dot{\mathbf{r}}+\left(\frac{1}{2G}\mathbf{r}+\frac{1}{3K}\mathbf{I}\right)\dot{p}$$

Where G and K are the pressure-dependent elastic shear and bulk moduli, respectively. Similarly, the hypoplastic response, i.e., the plastic strain rate $\dot{\boldsymbol{\varepsilon}}^p$, can be written as:

$$\dot{\boldsymbol{\varepsilon}}^p=\left(\frac{1}{H_r}\mathbf{n}_D+\frac{1}{3K_r}\mathbf{I}\right)(p\dot{\mathbf{r}}:\mathbf{n}_N) \qquad (2)$$
$$+\left(\frac{1}{H_p}\mathbf{r}+\frac{1}{3K_p}\mathbf{I}\right)h(p-p_m)\langle\dot{p}\rangle$$

where H_r and K_r are, respectively, the plastic shear and bulk moduli associated with the deviatoric stress ratio $\dot{\mathbf{r}}$; parameters H_p and K_p are, respectively, the plastic shear and bulk moduli associated with the pressure rate $\dot{p}$. The vectors $\mathbf{n}_D$ and $\mathbf{n}_N$ are unit vectors in stress space along the deviatoric part of $\dot{\boldsymbol{\varepsilon}}^p$ and the associated deviatoric loading direction, respectively. In this paper both $\mathbf{n}_D$ and $\mathbf{n}_N$ are taken to be the same as the unit vector normal to the maximum prestress memory bounding surface $\bar{f}=0$ (i.e., vector $\mathbf{n}$ in Figure 1). The p_m is the maximum value of mean pressure p experienced in past loading. The Heaviside step function $h(p-p_m)$ and the Macaulay brackets $\langle\ \rangle$ around $\dot{p}$ indicate that the plastic mechanism due to $\dot{p}$ operates only when $p=p_m$ and $\dot{p}>0$. As shown in Figure 1, the previous unloading stress point (i.e., $\boldsymbol{\alpha}$ in Figure 1), the current deviatoric stress ratio $\mathbf{r}$ and a properly defined 'image' stress $\bar{\mathbf{r}}$ on the maximum prestress memory bounding surface $\bar{f}(\boldsymbol{\sigma})=0$ are combined to determine variable plastic moduli H_r and K_r, which are continuous functions of the distance ρ from $\boldsymbol{\alpha}$ to $\mathbf{r}$ ($\rho=\|\mathbf{r}-\boldsymbol{\alpha}\|$) and the distance $\bar{\rho}$ from $\boldsymbol{\alpha}$ to $\bar{\mathbf{r}}$ ($\bar{\rho}=\|\bar{\mathbf{r}}-\boldsymbol{\alpha}\|$) (Dafalias 1986). It is worth mentioning that for practical applications, the shear-induced plastic strains usually dominate. Therefore the plastic strain rate $\dot{\boldsymbol{\varepsilon}}^p$ can be simplified as:

$$\dot{\boldsymbol{\varepsilon}}^p=\left(\frac{1}{H_r}\mathbf{n}+\frac{1}{3K_r}\mathbf{I}\right)(p\dot{\mathbf{r}}:\mathbf{n}) \qquad (3)$$

2 THE RESPONSE SENSITIVITY ALGORITHM BASED ON THE DIRECT DIFFERENTIATION METHOD

Response sensitivity is defined as the first derivative of a response quantity r (e.g., displacement, strain, stress) with respect to a sensitivity parameter θ, i.e., $dr/d\theta$. The sensitivity parameter could be a geometric, material or loading parameter. In general, the scalar response quantity $r(\theta) = r\left(\mathbf{f}(\theta), \theta\right)$ depends on the parameter θ both explicitly and implicitly through the vector function $\mathbf{f}(\theta)$. The DDM-based response sensitivities are computed after convergence of each time or loading step in nonlinear FE response analysis. This requires consistent differentiation of the FE algorithm for the response-only computation with respect to each sensitivity parameter θ. Consequently, the response sensitivity computation algorithm involves the various hierarchical levels of FE response analysis: (1) the structure/system level, (2) the element level or section level, and (3) the material level. Details about the DDM-based sensitivity formulations in classical displacement-based, force-based and mixed finite element methods can be found in the literature (Gu 2009, Scott et al. 2004, Haukaas & Der Kiureghian 2006).

2.1 *Displacement-based FE response sensitivity analysis using DDM*

After spatial discretization using the finite element method, the equations of motion of a structural system can be represented by the following nonlinear differential equation:

$$\mathbf{M}(\theta)\ddot{\mathbf{u}}(t,\theta) + \mathbf{C}(\theta)\dot{\mathbf{u}}(t,\theta) + \mathbf{R}(\mathbf{u}(t,\theta),\theta) = \mathbf{F}(t,\theta) \quad (4)$$

where t is time, θ is a scalar sensitivity parameter, $\mathbf{u}(t)$ is a vector of nodal displacements, $\mathbf{M}$ is the mass matrix, $\mathbf{C}$ is the damping matrix, $\mathbf{R}(\mathbf{u}, t)$ is a history-dependent internal resisting force vector, $\mathbf{F}(t)$ is the applied dynamic load vector, and $\dot{\mathbf{u}}$ and $\ddot{\mathbf{u}}$ denote, respectively, the first and second derivatives of $\mathbf{u}$ with respect to time. Without loss of generality, Eq. (4) can be integrated numerically using time-stepping methods such as the well-known Newmark-β method. The system of equations can be solved using the Newton-Raphson iteration procedure, which consists of solving a linearized system of equations at each iteration. In the following discretized format, a subscript n+1 is used to denote the variables at the time step n+1. Assuming that $\mathbf{u}_{n+1}$ is the converged solution for the current time step t_{n+1}, and recognizing that $\mathbf{R}(\mathbf{u}_{n+1}) = \mathbf{R}(\mathbf{u}_{n+1}(\theta),\theta)$ depends on θ explicitly and implicitly through $\mathbf{u}_{n+1}$, we obtain the following response sensitivity equation at the structural level using the chain rule of differentiation(Conte et al. 2003, Gu et al. 2009):

$$\begin{aligned}&\left[\frac{1}{\beta(\Delta t)^2}\mathbf{M} + \frac{\alpha}{\beta(\Delta t)}\mathbf{C} + (\mathbf{K_T})_{n+1}^{\text{stat}}\right]\frac{d\mathbf{u}_{n+1}}{d\theta} \\ &= \frac{d\tilde{\mathbf{F}}_{n+1}}{d\theta} - \left.\frac{\partial \mathbf{R}(\mathbf{u}_{n+1}(\theta),\theta)}{\partial\theta}\right|_{\mathbf{u}_{n+1}} \\ &\quad -\left(\frac{1}{\beta(\Delta t)^2}\frac{d\mathbf{M}}{d\theta} + \frac{\alpha}{\beta(\Delta t)}\frac{d\mathbf{C}}{d\theta}\right)\mathbf{u}_{n+1}\end{aligned} \quad (5)$$

where

$$\begin{aligned}\frac{d\tilde{\mathbf{F}}_{n+1}}{d\theta} &= \frac{d\mathbf{F}_{n+1}}{d\theta} + \frac{d\mathbf{M}}{d\theta}\left[\frac{1}{\beta(\Delta t)^2}\mathbf{u}_n + \frac{1}{\beta(\Delta t)}\dot{\mathbf{u}}_n - \left(1-\frac{1}{2\beta}\right)\ddot{\mathbf{u}}_n\right] \\ &\quad + \mathbf{M}\left[\frac{1}{\beta(\Delta t)^2}\frac{d\mathbf{u}_n}{d\theta} + \frac{1}{\beta(\Delta t)}\frac{d\dot{\mathbf{u}}_n}{d\theta} - \left(1-\frac{1}{2\beta}\right)\frac{d\ddot{\mathbf{u}}_n}{d\theta}\right] \\ &\quad + \frac{d\mathbf{C}}{d\theta}\left[\frac{\alpha}{\beta(\Delta t)}\mathbf{u}_n - \left(1-\frac{\alpha}{\beta}\right)\dot{\mathbf{u}}_n - (\Delta t)\left(1-\frac{\alpha}{2\beta}\right)\ddot{\mathbf{u}}_n\right] \\ &\quad + \mathbf{C}\left[\frac{\alpha}{\beta(\Delta t)}\frac{d\mathbf{u}_n}{d\theta} - \left(1-\frac{\alpha}{\beta}\right)\frac{d\dot{\mathbf{u}}_n}{d\theta} - (\Delta t)\left(1-\frac{\alpha}{2\beta}\right)\frac{d\ddot{\mathbf{u}}_n}{d\theta}\right]\end{aligned}$$

In Eq. (5), α and β are Newmark integration parameters, and $(\mathbf{K_T})_{n+1}^{\text{stat}}$ denotes the static algorithmic (consistent) tangent stiffness matrix of the structure/system, which is defined as the assembly of the consistent tangent stiffness matrices of the elements as

$$(\mathbf{K_T})_{n+1}^{\text{stat}} = \frac{\partial \mathbf{R}(\mathbf{u}_{n+1})}{\partial \mathbf{u}_{n+1}} = \mathop{\mathbf{A}}_{e=1}^{nel}\left(\int_{\Omega^e} \mathbf{B}^T \mathbf{C}_{n+1}^{alg} \mathbf{B}\, d\Omega^e\right) \quad (6)$$

where $\mathop{\mathbf{A}}_{e=1}^{nel}(\ )$ denotes the direct stiffness assembly operator, *nel* represents the number of elements in the FE model, $\mathbf{B}$ is the strain-displacement transformation matrix, $\mathbf{C}_{n+1}^{alg}$ denotes the algorithmic (consistent) tangent moduli obtained through consistent linearization of the constitutive law integration scheme (Simo & Hughes 1998), i.e.,

$$\mathbf{C}_{n+1}^{alg} = \frac{\partial \boldsymbol{\sigma}_{n+1}(\boldsymbol{\sigma}_n, \boldsymbol{\varepsilon}_n, \boldsymbol{\varepsilon}_{n+1}...)}{\partial \boldsymbol{\varepsilon}_{n+1}} \quad (7)$$

where $\boldsymbol{\sigma}_{n+1}$ is the stress at current time step t_{n+1}.
The second term on the right-hand side of Eq. (5) represents the partial derivative of the internal resisting force vector, $\mathbf{R}(\mathbf{u}_{n+1})$, with respect to the sensitivity parameter θ under the condition that the nodal displacement vector $\mathbf{u}_{n+1}$ remains fixed. It is computed through the direct stiffness assembly of the element resisting force derivatives as:

$$\left.\frac{\partial \mathbf{R}(\mathbf{u}_{n+1})}{\partial\theta}\right|_{\mathbf{u}_{n+1}} = \mathop{\mathbf{A}}_{e=1}^{nel}\left(\int_{\Omega^e} \mathbf{B}^{\mathrm{T}}(\mathbf{x}) \left.\frac{\partial \boldsymbol{\sigma}(\boldsymbol{\varepsilon}_{n+1}(\theta),\theta)}{\partial\theta}\right|_{\boldsymbol{\varepsilon}_{n+1}} d\Omega^e\right)$$

In this paper, the detailed derivation of the DDM based sensitivity equations and the consistent tangent operator of the bounding surface model is not shown, but can be found elsewhere (Gu & Wang 2013).

3 NUMERICAL EXAMPLE

In this section, an example is presented to verify the above DDM algorithm and illustrate its application in modeling liquefiable soils. The soils are considered fully saturated, and a simplified method is used to simulate the fluid-soil interaction: After the initial pressure is applied, the volume of each element is kept constant by fixing the vertical displacement of all nodes and imposing the same horizontal displacements to each pair of nodes at the same depth. This method is based on the following assumption: (a) The process of water seepage is much slower than that of the earthquake loading, thus can be ignored; (b) Volumetric modulus of water is much larger than that of soil, thus water is considered as incompressible. Based on these assumptions, the volume of water inside soil keeps constant during earthquake, and the volume of soil element is also constant. For a horizontal layered soil subject to horizontal earthquake loading, the total pressure at any point keeps constant and is equal to the initial pressure. Thus, the pore water pressure can be obtained as the difference between the initial pressure and the soil effective pressure, and it is not modeled as an independent variable. The soil effective pressure is computed by using the bounding surface soil model presented herein. Compared to using a fully coupled fluid-soil element, i.e., u-p formulation (ZienKiewicz & Chan 1999), the limitation of this approximation method is that it can not properly model the post-liquefaction process, which involves the water drainage and pore water pressure dissipation.

3.1 *Model description*

This example studies the response sensitivities of a multi-layered soil site located at Port Island, Kobe, Japan under earthquake loading. The soil there is composed of a layer of 18-m-thick reclaimed sand on top of silty clay, sand and silt layers. The soil profile is illustrated in Fig. 2. The top layer of reclaimed sand underwent extensive liquefaction, lateral spreading, and liquefaction-induced settlement during an earthquake on January 17, 1995. Ground motion acceleration time histories have been recorded using a downhole array with stations at the ground surface, at 16 m, 32 m, and 82 m below ground surface, providing valuable information for studying the liquefaction phenomenon (Elgamal et al. 1996).

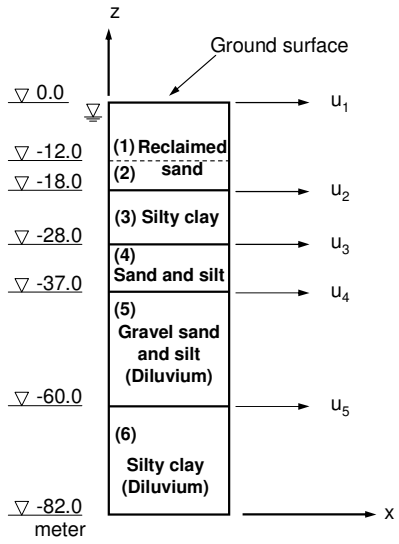

Figure 2. Soil profile at Port Island (Toki, 1995)

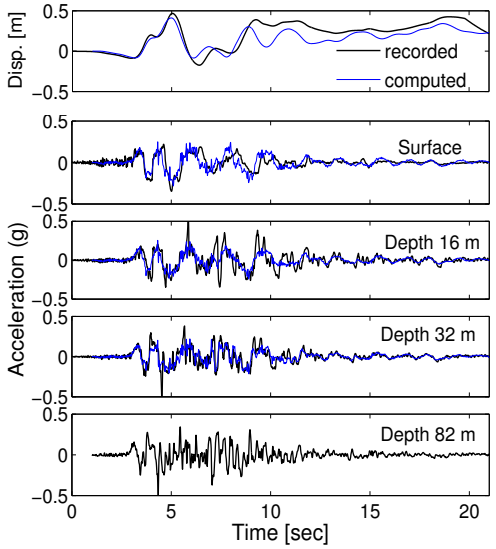

Figure 3 Displacement history at ground surface and acceleration histories at various depths

In this study, the soil column is discretized into a two-dimensional plane-strain finite element model consisting of 82 quadrilateral elements. The soil column deforms under the plane-strain simple-shear condition. The sand and clay materials are both modeled using the bounding surface model presented in this paper, and the material parameters are listed in (Gu & Wang 2013). Gravity is first applied statically, which generates the initial confining pressure within the soil column. The actual acceleration recorded using the downhole array at a depth of 82 m is applied to the base of the FE model, see Fig. 3. The Newmark-beta integration method is used with parameters $\alpha = 0.55$ and $\beta = 0.2756$ and a constant time step $\Delta t = 0.01$ sec. Good agreement is obtained between the recorded and computed horizontal displacement at the ground surface and between the recorded and computed accelerations at different soil depths, as can be seen in Fig.3. A typical shear stress vs. shear strain response and a typical shear stress vs. effective

confining pressure response in the top soil layer are shown in Fig.4. and Fig.5. respectively. During shaking, excessive pore-pressure builds up progressively in the reclaimed sands, resulting in reduced effective confining pressure. Liquefaction of the top layer occurs at about 10 seconds, as is evidenced by the significant loss of strength and stiffness of the soil material. These figures demonstrate that the numerical simulation agrees well with the real recorded data, and the presented bounding surface model is able to capture the key features of the sand behaviors including earthquake-induced liquefaction.

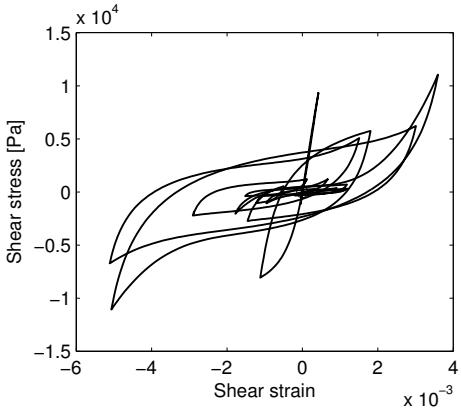

Figure 4. Shear stress vs. strain responses

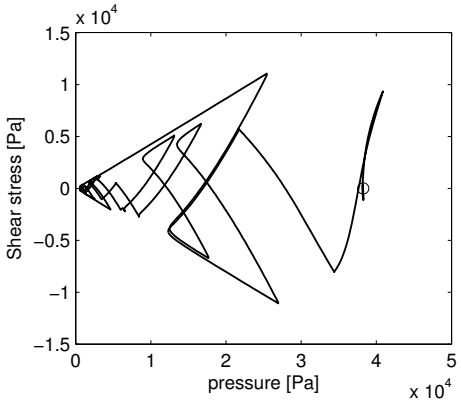

Figure 5 Shear stress vs. mean effective pressure response in top soil layer at a depth of 3.2 m

For practical interests, the sensitivity of the ground surface response to various material parameters of the top soil layer (i.e., layer #1) is investigated. The DDM-based response sensitivity results are verified using the FFD method with different levels of parameter perturbation and are shown in Figures 6 and 7. The FFD results are shown to converge asymptotically to the DDM results as the FFD perturbation reduces from 1e-1 and 1e-3 then 1e-5. Thus the DDM-based sensitivity algorithm and its implementation are verified to be correct for this multilayer soil system.

3.2 *Observations and findings*

The advantage of the DDM method over the FFD method is evident from the following error analysis. If the round-off error of $\mathbf{u}$ from FE analysis is δ, then the error of parameter sensitivity $(\partial\mathbf{u}/\partial\theta)\theta$ from the DDM method is also in the order of δ. However, the error from the FFD method consists of two parts: the round-off errors in the order of $O\left((\theta/\Delta\theta)\delta\right)$ where O is the Landau symbol; and the truncation error due to finite difference approximation is in the order of $O(\Delta\theta/\theta)M$, where $M=\theta^2\cdot\partial^2 u/\partial\theta^2(\xi)$ is a finite number, $\xi\in[\theta,\theta+\Delta\theta]$. When $\Delta\theta/\theta$ is large, the truncation error term dominates, and so the total error from the FFD method decreases as $\Delta\theta/\theta$ is reduced. On the other hand, when $\Delta\theta/\theta$ is small enough, the round-off error $O(\theta/\Delta\theta\,\delta)$ becomes dominant. In this case, reducing $\Delta\theta/\theta$ continuously will induce large round-off errors in the FFD results. The significant limitation of the FFD method can be observed but not shown in this paper.

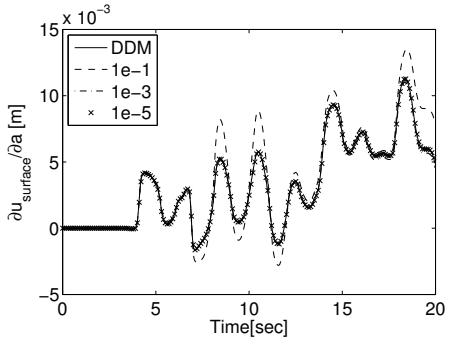

Figure 6. Sensitivity of ground surface displacement to parameter a obtained using DDM vs FFD with different levels of parameter perturbation

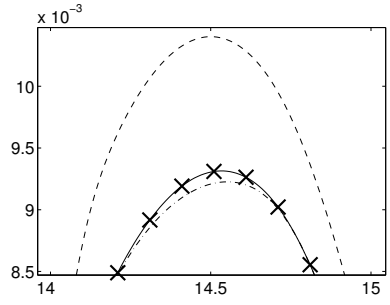

Figure 7. Zoomed view of Fig. 6

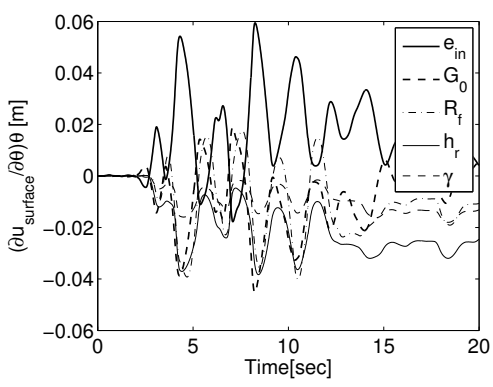

Figure 8. Relative importance of soil material parameters in regards to the horizontal displacement of the ground surface

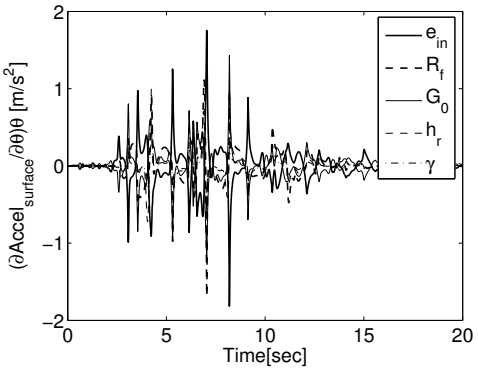

Figure 9 . Relative importance of soil material parameters in regards to the horizontal acceleration of the ground surface

The relative importance of system parameters to the system response can be quantified according to the peak absolute value of the normalized response sensitivity time history $\partial \mathbf{u}/\partial\theta\theta$. Fig. 8 shows the normalized sensitivities of the horizontal displacement response of the ground surface to the five most sensitive material parameters of the top soil layer. The order of importance of these parameters (in descending order) is as follows: (1) the initial void ratio e_{in}, (2) the model constant G_0, (3) the failure deviatoric stress ratio R_f, (4) the constant parameter h_r for the plastic shear modulus, and (5) the constant parameter γ for the critical state line. The void ratio e_{in} is identified as the most important parameter affecting the ground surface displacement response. From Fig. 8, one can see that most parts of the sensitivity histories $\left(\partial u_{surface}/\partial e_{in}\right)e_{in}$ are positive. Thus, reducing the void ratio will reduce the ground surface displacement. Fig. 9 shows the normalized sensitivities of the horizontal acceleration response of the ground surface to the five most sensitive parameters of the top soil. These results indicate that the ground surface acceleration is most sensitive to the same set of parameters as the ground surface displacement, except that the order of importance is slightly changed (in descending order) to (1) e_{in}, (2) R_f, (3) G_0, (4) h_r, and (5) γ. From these observations, it is clear that the initial void ratio e_{in} is the controlling parameter affecting significantly both ground surface displacement and acceleration during earthquake excitation.

4 CONCLUSION

The DDM method is a general, accurate and efficient method for computing FE response sensitivities to model parameters, especially in the case of nonlinear materials. This paper applies the DDM-based response sensitivity analysis methodology to a bounding surface plasticity material model that has been widely used to simulate nonlinear sandy soil behaviors under static and dynamic loading conditions. The algorithm is implemented in the general-purpose nonlinear FE analysis software OpenSees. The new algorithm and its software implementation are validated through two application examples, in which the DDM-based response sensitivities are compared with their counterparts obtained using FFD analysis. The advantage of the DDM method over the FFD method is also highlighted through convergence tests.

In the application example, the normalized response sensitivity analysis results are also used to measure the relative importance of the soil constitutive parameters in regards to the ground surface displacement and acceleration in the case of ground liquefaction. The example illustrates the use of finite element response sensitivity analysis to determine the relative importance of material parameters for specified system response parameters. The work presented in this paper significantly broadens the application of DDM-based response sensitivity analysis, since it enables numerous applications involving the use of the bounding surface plasticity material model. Work is underway to use the work presented here in response sensitivity analysis of large-scale nonlinear soil-structure interaction systems.

5 REFERENCES

Conte, J.P. 2003. Vijalapura PK, Meghella M. Consistent finite element response sensitivity analysis, *Journal of Engineering Mechanics*: 129(12): 1380-1393.

Dafalias, Y.F. 1986. Bounding surface plasticity. I: Mathematical foundation and hypoplasticity. *Journal of Engineering Mechanics*, 112(9): 966-987.

Der Kiureghian A, Haukaas T, Fujimura K. 2006. Structural reliability software at the University of California, Berkeley. *Structural Safety.* 28: 44-67.

Elgamal A, Zeghal M, Parra E. 1996. Liquefaction of reclaimed island in Kobe, Japan. *Journal of Geotechnical Engineering.* 122 (1): 39-49

Gu Q, Conte JP, Elgamal A, Yang Z. 2009. Finite element response sensitivity analysis of multi-yield-surface J2 plasticity model by direct differentiation method. *Computer Methods in Applied Mechanics and Engineering*. 198 (30-32): 2272-2285.

Gu Q, Barbato M, Conte JP. 2009. Handling of constraints in finite element response sensitivity analysis. *Journal of Engineering Mechanics.* 135(12): 1427-1438.

Gu Q, Barbato M, Conte JP, Li Y. 2010. OpenSees Command Language Manual --- Response Sensitivity Analysis based on the Direct Differentiation Method (DDM), http://opensees.berkeley.edu/wiki/index.php/Sensitivity_Analysis.

Gu Q. 2008. Finite element response sensitivity and reliability analysis of soil-foundation-structure-interaction systems,

Ph.D. Dissertation, Department of Structural Engineering, University of California, San Diego.

Gu Q., Wang G. 2013, Direct Differentiation Method for Response Sensitivity Analysis of a Bounding Surface Plasticity Soil Model. *Soil Dynamics and Earthquake Engineering*. Accepted Feb. 2013.

Haukaas T, Der Kiureghian A. 2006. Strategies for finding the design point in nonlinear finite element reliability analysis. *Journal of Probabilistic Engineering Mechanics.* 21 (2): 133-147.

Kleiber M, Antunez H, Hien TD, Kowalczyk V. 1997. Parameter Sensitivity in Nonlinear Mechanics: theory and finite element computations. Wiley.

Li XS. 2002. A sand model with state-dependent dilatancy. *Géotechnique*. 52 (3): 173-186.

McKenna F, Fenves GL. 2001. The OpenSees Command Language Manual, Version 1.2. Pacific Earthquake Engineering Research Center, University of California at Berkeley <http://opensees.berkeley.edu>.

Scott MH, Franchin P, Fenves GL, Filippou FC. 2004. Response sensitivity for nonlinear beam-column elements. *Journal of Structural Engineering*; 130(9): 1281-1288.

Simo JC. Hughes TJR. 1998. Computational Inelasticity. Springer-Verlag, New York.

Zhang Y, Der Kiureghian A. 1993. Dynamic response sensitivity of inelastic structures. *Computer Methods in Applied Mechanics and Engineering*; 108: 23-36.

Zienkiewicz OC, Chan AHC, Pastor M, Schrefler BA, 1999. Shiomi T. Computational Geomechanics with Special Reference to Earthquake Engineering, First Edition. Wiley.